Environment International 129 (2019) 461–469

Contents lists available at ScienceDirect

Environment International

journal homepage: www.elsevier.com/locate/envint

Methylmercury production in a paddy soil and its uptake by rice plants as affected by different geochemical mercury pools

Jinling Liu[a], Jianxu Wang[b,c,d,*], Yongqiang Ning[a], Shaochen Yang[a], Pengcong Wang[a], Sabry M. Shaheen[c,e,f], Xinbin Feng[b], Jörg Rinklebe[c,g]

[a] School of Earth Sciences, China University of Geosciences, Wuhan 430074, China
[b] State Key Laboratory of Environmental Geochemistry, Institute of Geochemistry, Chinese Academy of Sciences, Guiyang 550081, China
[c] University of Wuppertal, School of Architecture and Civil Engineering, Institute of Foundation Engineering, Water- and Waste-Management, Laboratory of Soil- and Groundwater-Management, Pauluskirchstraße 7, 42285 Wuppertal, Germany
[d] CAS Center for Excellence in Quaternary Science and Global Change, Xi'an 710061, China
[e] King Abdulaziz University, Faculty of Meteorology, Environment, and Arid Land Agriculture, Department of Arid Land Agriculture, 21589 Jeddah, Saudi Arabia
[f] University of Kafrelsheikh, Faculty of Agriculture, Department of Soil and Water Sciences, 33516 Kafr El-Sheikh, Egypt
[g] University of Sejong, Department of Environment, Energy and Geoinformatics, 98 Gunja-Dong, Guangjin-Gu, Seoul, South Korea

ARTICLE INFO

Handling Editor: Professor Adrian Covaci

Keywords:
Rice Hg pollution
MeHg accumulation
Health risk assessment
Geochemical Hg pools
Paddy field

ABSTRACT

The formation of neurotoxic methylmercury (MeHg) in paddy fields and its accumulation by rice plants is of high environmental concern. The contribution of different geochemical mercury (Hg) pools in paddy soils to MeHg production and its accumulation by rice seedlings is not well-studied up to now. Therefore, we investigated the impact of different inorganic Hg forms, including $HgCl_2$, nano-particulated HgS (nano-HgS), Hg bound with dissolved organic matter (Hg-DOM), β-HgS, and α-HgS, at levels of 5 mg Hg/kg soil and 50 mg Hg/kg soil, on the production of MeHg in the soil during rice growing season. Further, we studied the uptake of MeHg by the roots, stalks, leaves, and grains of rice in the tillering, panicle formation, and ripening growth stages, and compared these treatments to a non-polluted soil (control). MeHg contents in $HgCl_2$ polluted soil were the highest, and were 13.5 times and 36.1 times higher than control in 5 and 50 mg/kg Hg treatments, respectively. MeHg contents in α-HgS, β-HgS, nano-HgS, and Hg-DOM polluted soil were 3.9, 2.6, 2.4, and 1.7 times, and 4.4, 15.1, 6.7, and 10.9 times higher than control in 5 and 50 mg/kg Hg treatments, respectively, suggesting the mobilization and methylation of these Hg complexes. The ratio of MeHg to total Hg in the pore water (indication of methylation potential) in $HgCl_2$ and β-HgS treatments were higher than in Hg-DOM, α-HgS, and nano-HgS treatments. $HgCl_2$ treatment resulted in significantly higher MeHg contents in the root, stalk, leaf, and brown rice than nano-HgS, Hg-DOM, β-HgS, and α-HgS treatments both in 5 and 50 mg/kg Hg polluted soils. Rice grain in $HgCl_2$ treatment showed a potential hazard to human health, as indicated by high health risk index (HRI $>$ 1) of MeHg. Current results improve our understanding of MeHg production in soil polluted with different Hg forms, and the assessment of human health risks from consumption of MeHg-laden rice grain at Hg polluted sites with different Hg forms in soils.

1. Introduction

Mercury (Hg) and its compounds are toxic to humans, especially methylmercury (MeHg) which can be bioaccumulated and biomagnified in the aquatic food web, posing health risks to fish consumers (Driscoll et al., 2013). Besides fish consumption, recent studies also found a health risk associated with rice consumption in some regions of the world, especially in Asia (Liu et al., 2012; Antoniadis et al., 2017a, b, 2019). Like sediment, paddy fields are also MeHg production hotspots because of flooding during the rice growing season. MeHg can be more easily accumulated by rice grain than inorganic Hg (Meng et al., 2011). The high accumulation of MeHg in rice poses an ultimate risk to the food chain, and affects human health. Consumption of MeHg-contaminated rice is a major pathway for this toxic metal exposure to the rice consumers (Zhang et al., 2010a). Therefore, management of Hg polluted soils is important for the health of humans and ecosystems

* Corresponding author at: State Key Laboratory of Environmental Geochemistry, Institute of Geochemistry, Chinese Academy of Sciences, Guiyang 550082, China.
E-mail addresses: liujinling@cug.edu.cn (J. Liu), wangjianxu@vip.gyig.ac.cn (J. Wang), shaheen@uni-wuppertal.de, smshaheen@agr.kfs.edu.eg (S.M. Shaheen), rinklebe@uni-wuppertal.de (J. Rinklebe).

https://doi.org/10.1016/j.envint.2019.04.068
Received 11 December 2018; Received in revised form 15 April 2019; Accepted 28 April 2019
Available online 31 May 2019

(Wang C. et al., 2019; Wang et al., 2019a, b). An improved understanding of MeHg production in soils and its transfer from paddy fields to rice plants is crucial for a proper rice management.

MeHg production is mainly driven by Hg methylation microorganisms (Devai et al., 2005; Gilmour et al., 2013; Liu et al., 2014a; Beckers and Rinklebe, 2017), and mediated by multiple biogeochemical factors, such as redox potential, pH, dissolved organic matter (DOM), S^{2-}, as well as inorganic Hg bioavailability, etc. (Frohne et al., 2012; Rothenberg and Feng, 2012; Rothenberg et al., 2012; Liu et al., 2014a, b). Inorganic Hg pools serve as substrate for microbial methylation, and mainly consist of soluble Hg compounds (e.g., $HgCl_2$, $HgSO_4$), Hg sulfides (α-HgS, β-HgS, and nano-HgS), and Hg-DOM complex (Bernaus et al., 2006; Terzano et al., 2010; Wang et al., 2012a; Frohne and Rinklebe, 2013; Yin et al., 2016; Manceau et al., 2018; Wu et al., 2018).These inorganic Hg compounds differ in their mobility and resistance to methylation (Jonsson et al., 2014). Mercury sulfides are sparingly soluble, and display limited methylation potential in the environment compared to other Hg forms (Jonsson et al., 2014). However, the presence of aromatic organics can promote the dissolution of Hg sulfides by breaking its surface Hg−S bond (Waples et al., 2005). Nano-HgS is more amorphous than its well-crystallized form (β-HgS), which may be taken up by bacteria (e.g., *Escherichia coli*, *Bacillus subtillis*, *Geobacter sulfurreducens*) for methylation (Thomas et al., 2018). Mercury associated with DOM (Hg-DOM) may be more bioavailable for methylation relative to β-HgS (Jonsson et al., 2014). The extent to which Hg-DOM is subject to methylation is mediated by both the levels of sulfide (S^{2-}) and DOM (Deonarine and Hsu-Kim, 2009; Pham et al., 2014). When the concentration of S^{2-} is low, Hg is preferentially bound to DOM to form Hg-DOM complexes, which cannot cross the cell membrane for methylation (Deonarine and Hsu-Kim, 2009). In contrast, under high concentration of S^{2-}, DOM can increase the solubility of $HgS_{(S)}$ and limit its precipitation and aggregation, resulting in the formation of nano-HgS that may cross the cell membrane to be methylated (Waples et al., 2005; Pham et al., 2014).

Although much progress (e.g., Jonsson et al., 2012) has been made in our understanding of Hg methylation mechanisms, the knowledge gap of which inorganic Hg forms can be converted to MeHg in paddy fields and subsequently taken up by rice plants remains to be addressed. Therefore, our study was conducted to quantify the production of MeHg in paddy soils polluted by different inorganic Hg compounds, including $HgCl_2$, nano-HgS, Hg-DOM, β-HgS, and α-HgS, and characterize their contributions to rice plant MeHg, as well as assess the potential human health risks associated with MeHg in the rice grains. The results will provide new insights into the mechanisms of MeHg transfer in soil-rice system, and improve the management of Hg risks in paddy fields.

2. Material and methods

2.1. Preparation and characterization of the studied soil and inorganic Hg forms

The studied soil was collected from a rice paddy field in the suburbs of Wuhan city, Hubei province, China. The soil was air-dried, ground, passed through a 4 mm nylon sieve, and characterized for the basic soil properties. The average content of total Hg (THg) in the soil was 0.11 mg/kg, which was close to the average background levels of THg (0.10 mg/kg) in agricultural soil in China (Wang et al., 2016). The soil is a silty clay, weakly acidic with a pH of 6.8, and has 5.7% organic carbon. More information about the soil physical-chemical properties is provided in Table S1 in Appendix A.

We used $HgCl_2$, α-HgS, β-HgS, nano-HgS, and Hg-DOM as inorganic sources for soil pollution. The Hg-DOM and nano-HgS were synthesized using the methods documented by Zhang et al. (2012) and Gai et al. (2016). The characterization of nano-HgS, and the information for Hg-DOM synthesis are provided in chapter SI-1 in Appendix A. The X-ray diffraction (XRD) spectral of the nano-HgS is included in Fig. S1 (Appendix A) and indicated that the crystalline phase was dominated by meta-HgS. The $HgCl_2$ (ACS reagent, purity > 99.5%), α-HgS (Purity > 99%), and β-HgS powders (Purity > 99%) were purchased from Sigma-Aldrich.

2.2. Field plot experiments

We spiked each Hg compound at dosage of 5 and 50 mg/kg to non-polluted soil (THg = 0.11 ± 0.02 mg/kg (1σ)). These Hg levels were within previously reported ranges in agricultural soils (0.1 to > 10 mg/kg) at anthropogenic-impacted sites in China (Wang et al., 2016). Eleven 1.5 m^2 (1m × 1.5 m) plots at a site located close to Wuhan city, Hubei province, China were prepared for rice cultivation. Each plot was covered by Polyethylene films, and filled with 25 Kg of the ground soil. The DI water was used to flood the soil to reach a level of 2-cm above the soil surface. The calculated amount of each inorganic Hg compound ($HgCl_2$, α-HgS, β-HgS, nano-HgS, and Hg-DOM) was suspended in 3 L of purified water, and spiked into the soil plots at a dose of 5 mg/kg and 50 mg/kg, respectively (10 plots for Hg treatments). The soil and chemicals in each plot were mixed with an electronic stirrer for 20 min. A plot without Hg amendment was designated as control (THg = 0.11 ± 0.02 mg/kg (1σ)) (Table S1; Appendix A).Total Hg contents (THg) in the 5 mg/kg spiked soils ranged from 2.87 to 4.41 mg/kg, and the 50 mg/kg Hg soil treatments ranged from 35.7 to 58.7 mg/kg.

The hybrid rice cultivar Yangyou No.6, which is widely cultivated across central China, was chosen for our study. About 30-day old rice seedlings were transplanted to the experimental plots with 20 seedlings per plot on 1st June 2017. The rice seedlings were maintained for about 120 days. The purified water was provided regularly as required corresponding to the local weather during rice growing season. The Hg contributions from the irrigation water (THg = 2.51 ± 0.53 ng/L, n = 3; MeHg = 0.15 ± 0.02 ng/L, n = 3) were negligible. The agronomy management was performed using the same protocols as recommended by the local farmers.

2.3. Samples collection and analysis

The pH (Hanna Instruments Inc., USA) and oxidation reduction potential (ORP; FJA-6, China) of the overlying water were measured in situ prior to each sampling. The pore water, as well as rice plants and their paired soils were collected throughout rice growing season. The first, second, and third sampling was done on June 30, July 17, and September 5, 2017, respectively, corresponding to the rice plants growing stage of tillering, panicle formation, and ripening. The pore water samples were collected using a sediment core method, as documented in Liu et al. (2011). The sediment cores were collected from each plot, transported to the laboratory on ice, immediately centrifuged at 3000 rpm for 20 min, and then filtered with 0.45-μm pore-size membrane filter (Whatman, Whatman Inc., England). Pore water samples were divided into three subgroups, in which two subgroups were acidified with 2% HCl for THg and MeHg analysis and the third subgroup without acidification was kept for dissolved organic carbon (DOC) and sulfate analysis. All samples were stored at +4 °C in a refrigerator prior to analysis.

Three individual rice seedlings and their paired rhizosphere soils (about 10 to 20 cm in depth) were collected from each plot at each sampling campaign. Soil samples were stored in an ice-cooled container after collection, immediately transported to the laboratory, and stored in a deep freezer at −20 °C before freeze-drying. The soil samples were freeze-dried by a lyophilizer at −50 °C for 48 h, and were ground to powders using an agate mortar. The plant materials were first washed with tap water, and then rinsed with deionized water in an ultrasonic bath. After cleaning, the rice plants were divided into root, stalk, leaf, and panicle using stainless-steel scissors. The brown rice grains were further separated from panicles using a scalpel. All plant materials were

ground to powder by an electronic grinder.

Plant materials were digested with a fresh mixture of HNO_3/H_2SO_4 (v/v, 4:1) in a water bath at 95 °C for 3 h, and soil samples were digested with a fresh mixture of HCl and HNO_3 (v/v, 1:3) (Horvat et al., 1991; USEPA, 2002). The digested solutions and pore water samples were proceeded by BrCl oxidation, $SnCl_2$ reduction and purged into gold trap for Hg determination by cold vapor atomic fluorescence spectrometry (CVAFS, Brooks Rand Instruments, USA) (USEPA, 2002). For MeHg analysis, plant materials were digested using the KOH-methanol/solvent extraction technique, while soil samples were digested using the $CuSO_4$-methanol/solvent extraction technique, and pore water samples were distilled (Liang et al., 1996; USEPA, 1998). Then, MeHg in the solution was extracted with methylene chloride, back-extracted with water, and ethylated into methylethyl Hg, which was purged into a Tenax trap for MeHg analysis by CVAFS (CVAFS, Brooks Rand Instruments, USA) (USEPA, 1998). The concentration of sulfate and DOC was measured using an ion chromatograph (Dionex Aquion) and a TOC analyzer (Elementar Vario, Germany), respectively.

2.4. Human health risk assessment

The estimated human health risk index (HRI) of MeHg associated with rice grain (brown rice) ingestion was calculated using Eq. (1) (Jan et al., 2010; León-Cañedo et al., 2019).

$$HRI = C_m \times IR/b_w \times R_fD \quad (1)$$

where C_m is the concentration of MeHg (mg/kg dry weight basis) in the rice grains; IR is the average daily intake of rice (g/day); b_w is the body weight; HRI expresses the health risk of non-carcinogenic effects. A value lower than 1 means that population is safe, while a value higher than 1 indicates that population is at risk due to Hg consumption; R_fD represents the reference oral dose. The IR was assumed to be 176.6 g/day (Xu et al., 2017). The b_w value was taken as 61.8 kg for the Chinese population (Report on nutrition and chronic disease of Chinese residents, 2015), R_fD is 0.0001 mg/kg bw/day for MeHg, as recommended by USEPA (2017).

2.5. Data analysis and quality control and assurance

The method detection limits (3 × σ) were 0.002 ng/g for MeHg and 0.005 ng/g for THg in plant and soil samples. The relative standard deviation for analysis of duplicate samples was ≤10% for MeHg and THg. Recoveries for matrix spikes ranged from 80% to 107% for THg and MeHg. Certified reference materials (CRM), including the National Research Center for Certified Reference Materials rice standard GBW0858, and the Institute of Geophysical and Geochemical Exploration, China, soil standard GBW 07405, were used for quality control for rice plants and soil analysis. The recovery rates for THg and MeHg in these CRMs were provided in Table S2 (Appendix A).

The *SPSS* 17.0 software (SPSS Inc., USA) was used for statistical analysis. One-way analysis of variance (ANOVA) was used to test for significant differences between treatments. Pearson correlation analysis was used to test associations of MeHg in different rice plant tissues and pore water. Significant differences between treatment groups are denoted by different lower-case characters in the figures and tables.

3. Results and discussion

3.1. Impact of inorganic Hg forms on MeHg contents in the soils

The MeHg levels in the soils from different treatments and control throughout rice growing season are shown in Fig. 1. We observed significantly higher MeHg content in $HgCl_2$-treated soil than the others, both in 5 and 50 mg/kg Hg treatments throughout the tillering, panicle formation, and ripening growth stages. The presence of higher MeHg contents in $HgCl_2$-polluted soils as compared to Hg sulfides (α-HgS, β-HgS, and nano-HgS) and Hg-DOM polluted soils indicates a greater degree of methylation of $HgCl_2$ form than the other studied forms. $HgCl_2$ had the higher mobility than both Hg sulfides (β-HgS, α-HgS, and nano-HgS) and Hg-DOM, and became more bioavailable for microbial methylation by combing with organic molecules in soils (Jonsson et al., 2012, 2014). For instance, Hg-cysteine complexes formed by the binding of Hg(II) with cysteine, were bioavailable for *Geobacter sulfurreducens* (Schaefer and Morel, 2009).

The lower MeHg contents in Hg sulfide (α-HgS, β-HgS, and nano-HgS) treatments than the $HgCl_2$ treatment may reflect the limited mobility of Hg sulfides, as demonstrated by previous studies (Kim et al., 2003; Wang et al., 2012b). In Hg sulfides and Hg-DOM treatments, we found that MeHg content in the 5 mg/kg nano-HgS treatment was significantly ($P < 0.05$) higher than that in the 5 mg/kg Hg-DOM treatment at the tillering and ripening stages, and also higher than the 5 mg/kg α-HgS treatment at the ripening stage. There was no difference in MeHg content between the 5 mg/kg Hg sulfides and the Hg-DOM treatments at the panicle formation stage. In 50 mg/kg Hg treatments, we observed a significant higher MeHg content in β-HgS treatment than the other Hg sulfides treatments, as well as Hg-DOM treatment at the tillering stage. However, no significant difference in MeHg content was observed between Hg sulfides and Hg-DOM treatments in the panicle formation and ripening stages.

If we consider the average MeHg content in the control soil (1.0 ng/g; $n = 3$) throughout the rice growing season as the threshold MeHg pollution value, the MeHg contents in α-HgS, β-HgS, nano-HgS, and Hg-DOM polluted soils were 3.9, 2.6, 2.4, and 1.7 times higher, respectively than this threshold value in the 5 mg/kg treatments and 4.4, 15.1, 6.7, and 10.9 times higher, respectively than this threshold value in the 50 mg/kg Hg treatments. This suggests that these Hg pools, in particular β-HgS and Hg-DOM under 50 mg/kg Hg treatments, might be subject to mobilization, and subsequent methylation in paddy field soils. Further, we observed that the average MeHg contents in the soils polluted by both β-HgS and Hg-DOM increased with the levels of Hg spiked into the soil. For instance, the average MeHg contents in the 5 mg/kg β-HgS, and Hg-DOM treatments were 2.25 ng/g, and 0.95 ng/g, respectively, and 5.38 ng/g, and 3.15 ng/g in the 50 mg/kg β-HgS, and Hg-DOM treatments, respectively. This increase means that the mobilization and methylation of the two Hg species were affected by their dosages. In contrast to β-HgS and Hg-DOM treatments, MeHg content in α-HgS treatment decreased relatively with increasing Hg concentrations from 5 mg/kg to 50 mg/kg, but the variations were non-significant, perhaps due to the higher stability of α-HgS in the environment than β-HgS and Hg-DOM.

To further understand the behavior of Hg in different treatments, the concentrations of MeHg and THg in the pore water were analyzed.

3.2. Impact of inorganic Hg forms on MeHg and THg concentrations in the pore waters

The pore water MeHg concentrations in $HgCl_2$ treatments were obviously higher than the other treatments and control in both the 5 and 50 mg/kg Hg polluted soils (Table 1). These results were consistent with our observations for soil MeHg (Fig. 1). The MeHg concentrations in the pore water for the nano-HgS, Hg-DOM, β-HgS, and α-HgS polluted soils increased 1.52, 3.10, 3.04, and 3.42 times, and 8.52, 6.02, 5.56, and 6.77 times, respectively, for the 5 and 50 mg/kg Hg treatments, relative to control (Table S3, Appendix A). This means more mobilization and bioavailability of these Hg forms in the paddy fields, particularly at high concentrations. Unlike MeHg, THg concentrations in the pore water were higher in $HgCl_2$ and nano-HgS polluted soils as compared to that in Hg-DOM, α-HgS, and β-HgS polluted soils for the 5 mg/kg Hg treatments (Table 1). Particularly, in 50 mg/kg Hg treatments, nano-HgS treatment showed the highest THg concentrations in the pore water, followed by Hg-DOM, $HgCl_2$, β-HgS, and α-HgS treatments (Table 1). We found a similar level of THg in the pore waters for

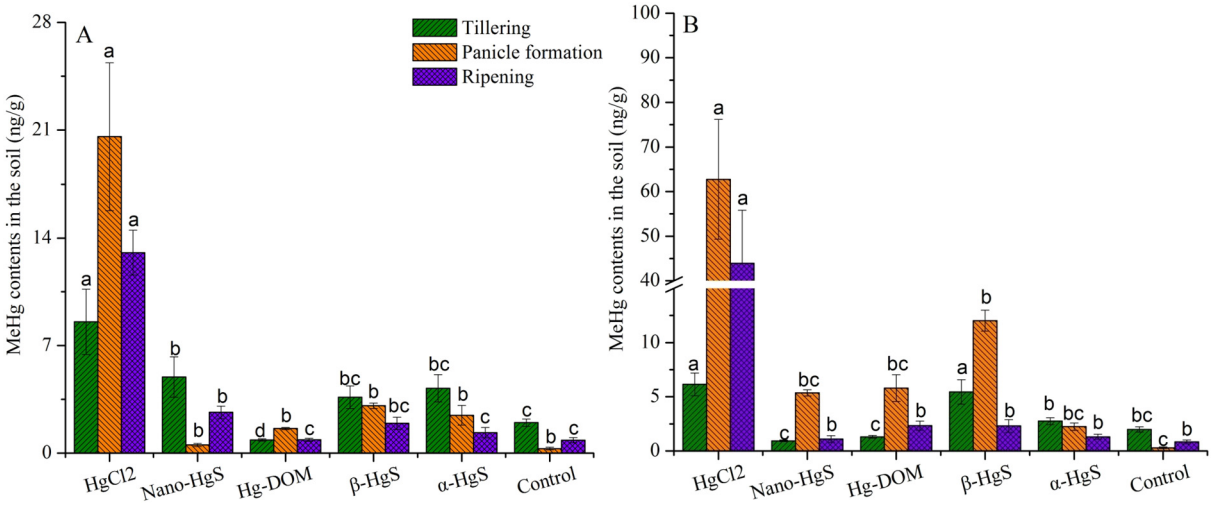

Fig. 1. MeHg contents in the paddy soil in $HgCl_2$, nano-particulated HgS (nano-HgS), Hg-DOM, β-HgS, and α-HgS treatments throughout rice growing season. A: 5 mg/kg Hg treatment; B: 50 mg/kg Hg treatment. The different lower-case character indicates that MeHg in the soil in five treatments significantly differed ($P < 0.05$). The error bar represents the standard deviation of the three replicates for each treatment ($n = 3$).

both the 5 and 50 mg/kg $HgCl_2$ treatments. The lack of apparent increase of THg concentrations in the higher Hg treatment levels might be attributed to the strong sorption of $HgCl_2$ by clay minerals in our soils (Miretzky et al., 2005) (Table S1, about 47.3% of soil particles had a diameter lower than 38-μm) and the high organic matter content (5.7%). The presence of higher concentrations of THg in the pore water in the Hg sulfide (i.e. α-HgS, β-HgS, and nano-HgS) and Hg-DOM treatments (particularly nano-HgS and Hg-DOM) than control, in 50 mg/kg Hg treatment may indicate their mobilization under high concentrations in the paddy field throughout the rice growing season.

3.3. Mechanisms of nano-HgS, Hg-DOM, α-HgS and β-HgS mobilization in the soils

Nano-HgS treatments showed relatively high concentrations of THg in the pore water as compared to both α-HgS and β-HgS treatments, particularly at the higher treatment levels (i.e. 50 mg/kg), suggesting that it is more mobile relative to α-HgS and β-HgS (Deonarine and Hsu-Kim, 2009). It has been reported that nano-HgS is stable and persists in the environments under anoxic conditions, but becomes unstable in the presence of sunlight and oxic environments as a consequence of the photo-induced changes or oxidation of organic matter adsorbed on the surface of nano-HgS (Mazrui et al., 2018). Paddy fields are exposed to sunlight and drained to become oxic, by which the stability of nano-HgS might be affected and subsequently be solubilized (Mazrui et al., 2018). The redox potential in the overlying water in our soils ranged from +74 to +143 mV, +120 to +163 mV, and +282 to +324 mV at the tillering, pancile formation, and ripening stages, respectively (Table S4; Appendix A), suggesting moderately aerobic conditions at the tillering, and strongly aerobic at the panicle and ripening stages. Thus the dissolution of nano-HgS might occur under these aerobic conditions (Mazrui et al., 2018). Further, Nano-HgS might be dissolved and disaggregated in the presence of DOC or organic sulfur compounds and (re)precipitated by S^{2-} in solution over periods of hours to days (Ravichandran et al., 1999; Slowey, 2010).

Hg-DOM-treated soils showed lower THg concentration (200–300 μg/L) in the pore water than nano-HgS (100–1220 μg/L) and $HgCl_2$ treatments (100–2950 μg/L), but a similar level with α-HgS treatment (180–330 μg/L) (Table 1). This suggests that most Hg-DOM complexes might be transformed to more stable forms in our soil. Manceau et al. (2015) found that about 74% of Hg in Hg-DOM (Hg coordinated to two sulfur atoms) progressively formed poorly crystalline HgS in the solution after incubation for 6 months. It appears that Hg-DOM complexes, particularly those in which Hg coordinated to sulfur atoms, tend to be transformed to HgS in the environment. Our Hg-DOM complexes were incubated over 4 months in the soil; it is thus likely that most of them (probably coordinated to sulfur atoms) might be transformed to HgS. The relatively higher THg concentration in Hg-DOM treatments relative to non-treated control suggests that partial Hg-DOM was mobilized, probably through decomposition of DOM by microorganisms (Bajracharya et al., 2016), and desorption of Hg^{2+} from unstable Hg-DOM complexes (Skyllberg et al., 2000). It is reported

Table 1
Methylmercury (MeHg) and total Hg concentrations (THg), as well as their ratios in the pore water in $HgCl_2$, nano HgS, Hg-DOM, β-HgS, and α-HgS treatments throughout trice growing season ($n = 3$).

Hg Levels	Treatments	THg (μg/L)		MeHg (μg/L)		MeHg/THg (%)	
		Range	Average	Range	Average	Range	Average
0.11 mg/kg	Control	37–257	114	0.42–0.53	0.48	0.14–1.43	0.76
5 mg/kg	$HgCl_2$	100–2950	1190	4.10–29.2	12.6	0.74–4.40	2.05
	Nano-HgS	100–1220	500	0.45–1.18	0.73	0.09–0.45	0.28
	Hg-DOM	200–300	250	1.04–1.89	1.49	0.51–0.74	0.59
	β-HgS	40–290	200	0.37–2.64	1.46	0.14–6.56	2.38
	α-HgS	180–330	260	0.51–3.12	1.64	0.16–1.11	0.66
50 mg/kg	$HgCl_2$	380–2040	960	9.42–56.4	30.3	2.48–5.35	3.53
	Nano-HgS	260–3040	1470	2.38–6.58	4.09	0.11–0.93	0.55
	Hg-DOM	740–1840	1200	2.10–4.48	2.89	0.11–0.60	0.31
	β-HgS	80–1190	510	1.22–3.44	2.67	0.29–4.01	1.58
	α-HgS	200–400	320	1.82–4.72	3.25	0.85–1.17	0.97

that Hg binds strongly to thiols in DOM at Hg to DOM ratios below about 1 μg of Hg/mg of DOM, while some fraction of Hg weakly binds to oxygen functional groups at Hg/DOM ratios above about 10 μg of Hg/mg of DOM (Haitzer et al., 2002). In our study, we synthesized the Hg-DOM with a Hg to DOM molar ratio of 2.5 μmol Hg/μmol DOM, and thus some Hg may be coordinated to O atoms. These Hg-DOM complexes may have been unstable because of the weak bond between Hg and DOM.

The mobilization of α-HgS and β-HgS, particularly at the higher treatment levels (i.e. 50 mg/kg), may be linked to the DOC effect, as the DOC, particularly those with high aromaticity (Waples et al., 2005), were able to dissolve Hg sulfides by complexation of Hg and oxidation of surface sulfur species (Ravichandran et al., 1998). Also, this oxidative HgS dissolution can acidify the solution as shown in Eq. (2) (Holley et al., 2007).

$$HgS(s) + 2O_2(aq) + 2H_2O \leftrightarrow Hg(OH)_2(aq) + SO_4^{2-} + 2H^+ \quad (2)$$

We found a similar phenomenon in our α-HgS- and β-HgS-treated soils. For instance, in 5 mg/kg Hg treatment the average pH values in α-HgS- and β-HgS-treated soils were 6.63 and 6.79, respectively (n = 3), which decreased 0.43 and 0.27 units compared to the non-polluted soil (7.06) (Table S4; Appendix A). As a comparison, the pH value in $HgCl_2$-treated soils was 6.91, close to that of the non-polluted control soil.

Although $HgCl_2$ was soluble, treated soils showed relatively low Hg concentrations, even at a level close to that in 50 mg/kg nano-HgS treatment. We attributed this phenomenon to the appearance of biogeochemical reactions such as reduction, complexation, and adsorption for $HgCl_2$ (Bollen et al., 2008; Zhu et al., 2018; Shetaya et al., 2019), leading to the decrease of mobility of this form.

The ratio of MeHg to THg in the pore water was calculated to indicate methylation potential (Table 1). The average value of this ratio of different Hg forms in both 5 and 50 mg/kg Hg treatments followed the order: $HgCl_2$ > β-HgS > α-HgS > nano-HgS > Hg-DOM, $HgCl_2$ ≈ β-HgS > α-HgS > Hg-DOM > nano-HgS, respectively. It showed that $HgCl_2$ and β-HgS have higher methylation ratios than Hg-DOM, α-HgS, and nano-HgS, which is consistent with our soil MeHg content results (Fig. 1). Although nano-HgS and Hg-DOM treatments led to higher THg concentrations in the pore water than α-HgS and β-HgS treatments, they showed lower MeHg to THg ratios (Table 1), likely suggesting that partially mobilized Hg from these treatments were not bioavailable for microbial methylation. We attributed this observation to the presence of colloidal HgS in the pore water because the mobilization of nano-HgS might form colloidal HgS (Slowey, 2010), and Hg-DOM might form Hg-S-DOM complexes which also tended to be transformed to colloid HgS through aggregation processes (Hsu-Kim et al., 2013). Colloidal HgS that is smaller than the filter pore (0.45-μM pore size) may be mischaracterized as “soluble” (Ravichandran et al., 1999), but have limited bioavailability for methylation.

We found significant correlations between ln(MeHg/THg) ratio and ln(DOC) both in 5 and 50 mg/kg Hg treatments (Fig. 2), suggesting a positive role of DOC in Hg methylation. Poor correlations between ln(MeHg/THg) and ln(SO_4^{2-}) may indicate the impact of sulfate on Hg methylation was minor (Fig. 2), or it play a more complex role in our study. It seems that Hg methylation in our soils might be affected by both THg and DOC. The integrated effect of DOC and THg on methylation potential is shown using a triple figure. As shown in Fig. S2, the highest Hg methylation potential occurred in the soils with ln(DOC) of 3.6 and ln(THg) of 7.7 (with $HgCl_2$ and β-HgS treatments).

3.4. Distribution of MeHg in the rice plants

The MeHg contents in the roots, stalks, and leaves of rice in the tillering, panicle formation, and ripening growing stages are shown in Fig. 3. The MeHg contents in the roots, stalks, and leaves of rice plants were obviously higher in the 50 mg/kg Hg treatments than the 5 mg/kg Hg treatments. These results demonstrated that MeHg in soils is the primary source of its accumulation in rice plants (Liu et al., 2012; Xing et al., 2019). The $HgCl_2$ treatment led to significantly higher MeHg contents in the roots, stalks, and leaves of rice plants than the Hg-DOM, nano-HgS, β-HgS, and α-HgS treatments at both treatment levels (Fig. 3). The levels of MeHg in the leaves (Fig. 3-A, -D) and stalks (Fig. 3-B, -E) of rice in our study were close to the results from previous investigations of MeHg distribution in rice plants collected from Hg-polluted sites in China (Feng et al., 2007; Zhang et al., 2010a; Liu et al., 2012). MeHg in the leaves of rice plants both in 5 and 50 mg/kg Hg treatments varied with the Hg forms spiked to the soil. For instance, MeHg contents in 5 mg/kg β-HgS and α-HgS treatments were higher than that in the nano-HgS, and Hg-DOM treatments, as well as control, at the tillering and ripening stages, respectively. MeHg contents in the leaves of rice plants in the 50 mg/kg β-HgS and nano-HgS treatments were higher than that in the Hg-DOM and α-HgS treatments, as well as control. MeHg contents in the stalks in both 5 and 50 mg/kg β-HgS treatments were higher than the other Hg sulfides and Hg-DOM treatments, as well as control at the panicle formation and tillering stages, respectively. MeHg contents in the roots were higher both in the 5 and 50 mg/kg β-HgS treatments than the other Hg sulfides and Hg-DOM treatments, as well as control at the tillering stage (Fig. 3-C, -F). It seems that more MeHg accumulated in the tissues of rice plants in β-HgS treatment compared to the other Hg sulfides and Hg-DOM treatments, perhaps due to the relatively higher MeHg contents in the soils

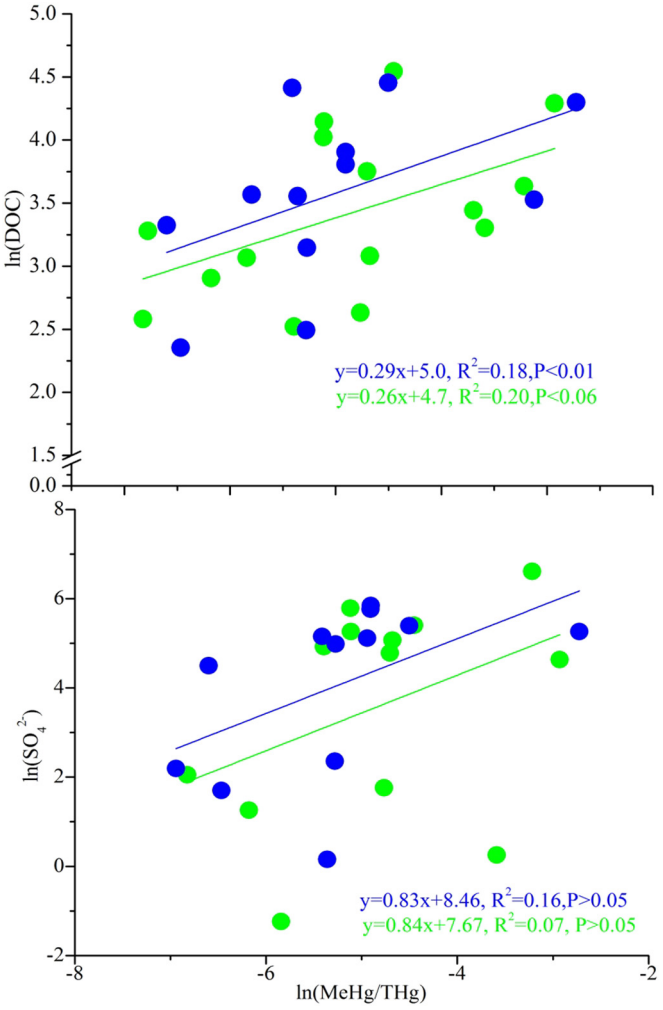

Fig. 2. Relationship between ln(MeHg/THg) and ln(DOC), and ln(SO_4^{2-}).The blue filled circles indicate 5 mg/kg Hg treatment; The green filled circles indicate 50 mg/kg Hg treatment. (For interpretation of the references to color in this figure legend, the reader is referred to the web version of this article.)

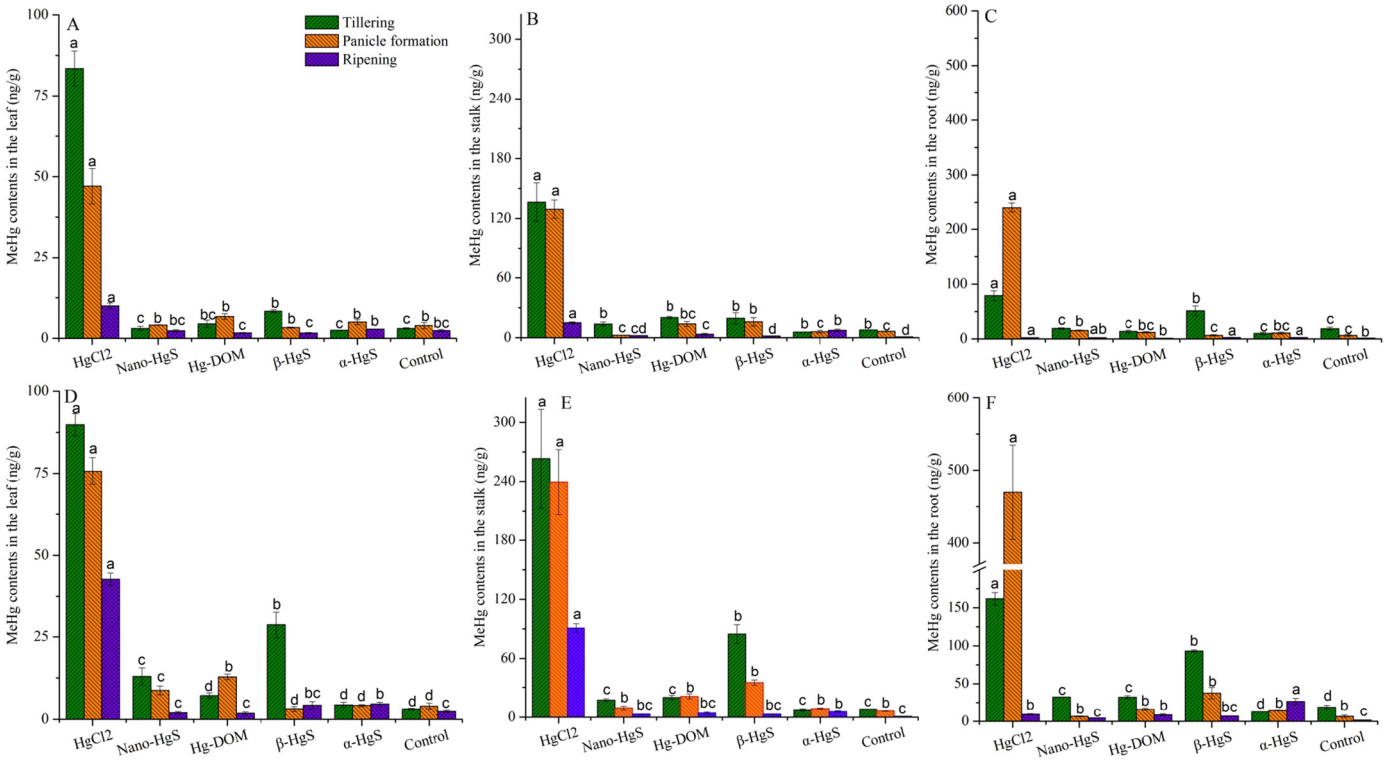

Fig. 3. Distribution of MeHg in the leaf, stalk, and root of rice plants in $HgCl_2$, nano-HgS, Hg-DOM, β-HgS, and α-HgS treatments throughout rice growing season. A, B, C: 5 mg/kg Hg treatments; D, E, F: 50 mg/kg Hg treatments. The different lower-case character indicates that MeHg in the soil in five treatments significantly differed ($P < 0.05$) at each sampling time.

relative to the other Hg sulfides and Hg-DOM treatments, as well as control (Fig. 1-A, -B).

We observed a trend of decreasing of MeHg content in both leaf and stalk as a function of sampling times in all the treatments. For instance, MeHg content in the leaf of rice grown in 5 mg/kg $HgCl_2$ polluted soil was 83 ng/g at the tillering stage, and it decreased to 47 ng/g and 10 ng/g at the panicle formation and ripening stages, respectively. We attributed this phenomena to the translocation of MeHg from the leaf and stalk to the grain at the ripening stage, and this translocation process may be associated with nutrient movement (e.g., translocation) from the stalk and leaf to the grain (Meng et al., 2011). Supporting this, we found a strong positive correlation between MeHg contents in the brown rice and that in leaf ($r = 0.94$) and stalk ($r = 0.92$; Table S5; Appendix A).

MeHg content in the brown rice is of greatest concern because it was the major tissue of rice plant that is utilized for human consumption. Brown rice MeHg contents were significantly higher in $HgCl_2$ treatment than the other treatments and varied from 51.6 ng/g in 5 mg/kg $HgCl_2$ to 99 ng/g in 50 mg/kg $HgCl_2$ treatment (Fig. 4-A, -B). These values were about 2.6 to 5 times over the maximum allowable THg in rice grain (< 20 ng/g, GB2762-2012) set by the Chinese government, indicating a high health risk. MeHg contents in the brown rice in Hg-DOM, β-HgS, nano-HgS, and α-HgS treatments ranged between 7 and 14 ng/g in 50 mg/kg Hg treatment, and between 3.3 and 7.6 ng/g in 5 mg/kg Hg treatment, respectively, which were higher than that in the brown rice (2.4 ng/g, $n = 3$) grown in non-polluted soil, suggesting a MeHg contamination in the grain of rice plants in these treatments. MeHg content in the brown rice in 50 mg/kg Hg-DOM, β-HgS, nano-HgS, and α-HgS polluted soils increased by 44%, 114%, 68%, and 337% as compared to that in 5 mg/kg Hg treatments, suggesting a potential risk associated with rice grain MeHg in the presence of high Hg contents in soils. The MeHg in the pore water could be the main source for MeHg in the rice tissues, as demonstrated by a noticeable positive correlation between MeHg content in the pore water and that in the leaf, stalk, and brown rice (Table S5; Appendix A). These results are consistent with prior observations that the soil is the dominant source of MeHg to rice seedlings (Zhang et al., 2010b; Liu et al., 2012; Xing et al., 2019). Thus, the mobilization and methylation of different inorganic Hg pollutants determines MeHg accumulation by the rice plants.

4. Health risk assessment of MeHg by intaking rice grain

The HRIs of MeHg for rice grain in 5 mg/kg $HgCl_2$, nano-HgS, Hg-DOM, β-HgS, and α-HgS treatments were 1.48, 0.14, 0.14, 0.22, and 0.09, respectively, and in 50 mg/kg $HgCl_2$, nano-HgS, Hg-DOM, β-HgS, and α-HgS treatments was 2.83, 0.21, 0.31, 0.37, and 0.89, respectively (Fig. 5). These values were higher than control (0.07), suggesting a potential health risk associated with these treatments. Furthermore, the HRI values from $HgCl_2$ treatments exceeded the safe standard of 1.0 recommended by USEPA (2017), suggesting a high health risk associated with rice grown in $HgCl_2$ polluted soils with contents of 5–50 mg/kg. Based on these results, we estimated a high risk associated with those rice plants grown in $HgCl_2$-polluted soil, since their grains may accumulate abnormally high levels of MeHg, posing high health risk to the consumers. For instance, soil polluted by Chlor-alkali plant activities usually contained a large fraction of $HgCl_2$ (Wang et al., 2019a, b, c), and the cultivation of rice at these sites could potentially result in a greater environmental risk for rice grain Hg accumulation.

Although the HRIs of MeHg for rice grain in both 5 and 50 mg/kg nano-HgS, Hg-DOM, β-HgS, and α-HgS treatments were lower than 1, their risks should not be underestimated. The HRIs of MeHg for these treatments increased as a function of the Hg content in the soils, suggesting that MeHg in the rice grains grown in soils with high Hg contents may be hazardous to human health. Mercury speciation in these treatments was generally considered to be of limited bioavailability, and most immobilization techniques focus on the conversion of bioavailable Hg to Hg-sulfides in order to mitigate the pollution risk (Wang et al., 2012a, 2018, 2019a, b), particularly for Hg-polluted paddy fields.

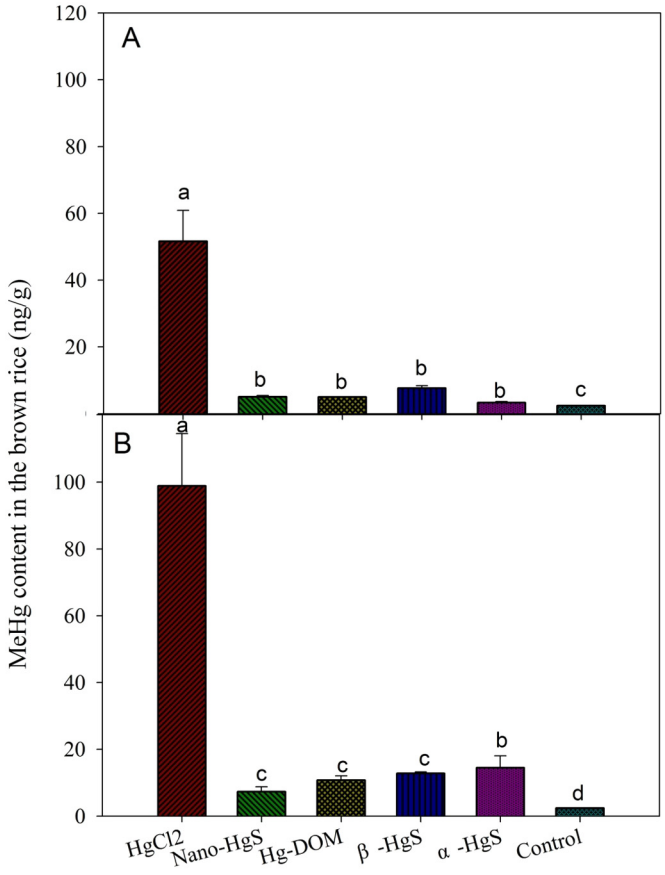

Fig. 4. Distribution of MeHg in the brown rice of rice plants in $HgCl_2$, nano-HgS, Hg-DOM, β-HgS, and α-HgS treatments throughout rice growing season. A: 5 mg/kg Hg treatment; B: 50 mg/kg Hg treatment. The different lower-case character indicates that MeHg in the soil in five treatments significantly differed ($P < 0.05$) at each sampling time.

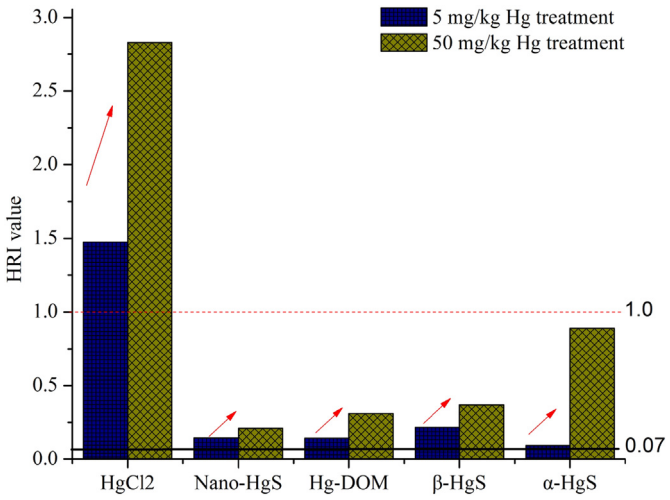

Fig. 5. The estimated human health risk index (HRI) of MeHg of rice grain (brown rice) in $HgCl_2$, nano-HgS, Hg-DOM, β-HgS, and α-HgS treatments. The red arrows above the green column mean that the HRI value increased in 50 mg/kg Hg treatments compared to that in 5 mg/kg Hg treatments. The red dash line in the figure indicates the boundary for evaluating the safety of the population. (For interpretation of the references to color in this figure legend, the reader is referred to the web version of this article.)

This may cause unexpected risks to the food chain in case of the cultivation of rice at these sites. In addition, the Hg sulfides (e.g., β-HgS, nano-HgS, and α-HgS) and Hg-DOM predominantly occurred in most Hg polluted soils in the world (Biester and Scholz, 1997; Wang et al., 2012b). For example, β-HgS and nano-HgS dominated in the soils polluted by Hg mining activities (Yin et al., 2016; Manceau et al., 2018), and the high proportion of Hg-DOM and HgS presented in floodplain soils and wastewater-irrigated soils (Frohne and Rinklebe, 2013; Wu et al., 2018). The high risk may be presented at these sites with rice cultivation.

5. Conclusions

$HgCl_2$ treatments resulted in higher MeHg contents in the soil and pore water, relative to nano-HgS, Hg-DOM, β-HgS, and α-HgS treatments. Furthermore, the relatively high THg concentrations in the pore water of Hg sulfides (particularly nano-HgS) and Hg-DOM treatments compared to the non-polluted control soil suggested the mobilization of Hg from these Hg complexes. Both $HgCl_2$ and β-HgS treatments showed higher MeHg to THg ratio (methylation potential) relative to nano-HgS, Hg-DOM, and α-HgS treatments. MeHg contents in the tissues of rice followed the order: $HgCl_2$ > β-HgS > nano-HgS ≈ Hg-DOM ≈ α-HgS throughout the rice growing season. Rice grown in $HgCl_2$ polluted soil with low (e.g., 5 mg/kg) or high (e.g., 50 mg/kg) levels of THg accumulated higher MeHg contents in their grains relative to other treatments. Rice grain MeHg levels increased with the THg levels in β-HgS, nano-HgS, α-HgS and Hg-DOM treatments, suggesting a potential risk of grain MeHg in those heavily polluted soils. There was a high health risk from MeHg for rice grains in $HgCl_2$ treatments, as indicated by their HRI values (1.48–2.83). Although the HRI values of MeHg of rice grain in nano-HgS, Hg-DOM, β-HgS, and α-HgS treatments were below 1, the health risks should not be ignored because the HRI values seem to increase with the Hg contents in the soils.

Our results demonstrate a high risk of $HgCl_2$ in paddy fields since it may accumulate in rice grain. These results may be helpful for assessing Hg risk and managing polluted soils at chlor-alkali plants, where $HgCl_2$ is the dominant species in soils. Growing rice in the presence of high levels of Hg sulfides and Hg-DOM should also warrant attention since these Hg pollutants can be mobilized, methylated, and subsequently accumulate in rice grain to unacceptable levels, causing risks to humans.

Acknowledgments

This work was financially supported by the National Natural Science Foundation of China [grant no 41573082, 41773112, 41703116]; the Fundamental Research Funds for the Central Universities, China University of Geosciences, Wuhan [grant no CUGCJ1703, CUG170104, CUGQYZX1707]; the Opening Fund of the China Merchants Chongqing Communications Technology Research & Design Institute Co., LTD [no. GSGZJ-2015-06]; the State Key Laboratory of Environmental Geochemistry [grant no SKLEG2015903, SKLEG2017907, SKLEG2017912]. We also thank the German Alexander von Humboldt Foundation for the financial support of the postdoctoral fellowship of Dr. Jianxu Wang (Ref 3.5-1186537-CHN-HFST-P) and the experienced researcher's fellowship of Prof. Dr. Shaheen (Ref 3.4 - EGY - 1185373 - GF-E) at the University of Wuppertal, Germany.

Appendix A. Supplementary data

Supplementary data to this article can be found online at https://doi.org/10.1016/j.envint.2019.04.068.

References

Antoniadis, V., Shaheen, S.M., Boersch, J., Frohne, T., Du Laing, G., Rinklebe, J., 2017a.

Bioavailability and risk assessment of potentially toxic elements in garden edible vegetables and soils around a highly contaminated former mining area in Germany. J.Environ. Manage. 186, 192–200.
Antoniadis, V., Levizou, E., Shaheen, S.M., Ok, Y.S., Sebastian, A., Baum, C., Prasad, M.N., Wenzel, W.W., Rinklebe, J., 2017b. Trace elements in the soil-plant interface: phytoavailability, translocation, and phytoremediation-a review. Earth-Sci.Revi. 171, 621–645.
Antoniadis, V., Shaheen, S.M., Levizou, E., Shahid, M., Niazi, N.K., Vithanage, M., Ok, Y.-S., Bolan, N., Rinklebe, J., 2019. A critical prospective analysis of the potential toxicity of trace element regulation limits in soils worldwide: are they protective concerning health risk assessment? - a review. Environ. Int. https://doi.org/10.1016/j.envint.2019.03.039.
Bajracharya, U., Feng, X., Jackson, B., 2016. Mercury retention in soil in association with organic matter decomposition and sulfur cycle. In: AGU Fall Meeting Abstracts.
Beckers, F., Rinklebe, J., 2017. Cycling of mercury in the environment: sources, fate, and human health implications: a review. Crit. Rev. Environ. Sci. Technol. 47, 693–794.
Bernaus, A., Gaona, X., van Ree, D., Valiente, M., 2006. Determination of mercury in polluted soils surrounding a chloralkali plant: direct speciation by X-ray absorption spectroscopy techniques and preliminary geochemical characterization of the area. Anal.Chim. Acta 565, 73–80.
Biester, H., Scholz, C., 1997. Determination of mercury binding forms in contaminated soils: mercury pyrolysis versus sequential extractions. Environ. Sci. Technol. 31, 233–239.
Bollen, A., Wenke, A., Biester, H., 2008. Mercury speciation analyses in $HgCl_2$-contaminated soils and groundwater-implications for risk assessment and remediation strategies. Water Res. 42, 91–100.
Deonarine, A., Hsu-Kim, H., 2009. Precipitation of mercuric sulfide nanoparticles in NOM-containing water: implications for the natural environment. Environ. Sci. Technol. 43 (7), 2368–2373.
Devai, I., Patrick, W.H., Neue, H.U., DeLaune, R.D., Kongchum, M., Rinklebe, J., 2005. Methyl mercury and heavy metal content in soils of Rivers Saale and Elbe (Germany). Anal. Lett. 38, 1037–1048.
Driscoll, C.T., Mason, R.P., Chan, H.M., Jacob, D.J., Pirrone, N., 2013. Mercury as a global pollutant: sources, pathways, and effects. Environ. Sci. Technol. 47, 4967–4983.
Feng, X., Li, P., Qiu, G., Wang, S., Li, G., Shang, L., Meng, B., Jiang, H., Bai, W., Li, Z., 2007. Human exposure to methylmercury through rice intake in mercury mining areas, Guizhou Province. China. Environ. Sci. Technol 42, 326–332.
Frohne, T., Rinklebe, J., 2013. Biogeochemical fractions of mercury in soil profiles of two different floodplain ecosystems in Germany. Water Air Soil Pollut. 224 (6), 1591–1595.
Frohne, T., Rinklebe, J., Langer, U., Du Laing, G., Mothes, S., Wennrich, R., 2012. Biogeochemical factors affecting mercury methylation rate in two contaminated floodplain soils. Biogeosciences 9, 493–507.
Gai, K., Hoelen, T.P., Hsu-Kim, H., Lowry, G.V., 2016. Mobility of four common mercury species in model and natural unsaturated soils. Environ. Sci. Technol. 50 (7), 3342–3351.
Gilmour, C.C., Podar, M., Bullock, A.L., Graham, A.M., Brown, S.D., Somenahally, A.C., Johs, A., Hurt, R.A., Bailey, K.L., Elias, D.A., 2013. Mercury methylation by novel microorganisms from new environments. Environ. Sci. Technol. 47, 11810–11820.
Haitzer, M., Aiken, G.R., Ryan, J.N., 2002. Binding of mercury(II) to dissolved organic matter: the role of the mercury-to-DOM concentration ratio. Environ. Sci. Technol. 36, 3564–3570.
Holley, E.A., James Mc Quillan, A., Craw, D., Kim, J.P., Sander, S.G., 2007. Mercury mobilization by oxidative dissolution of cinnabar (α-HgS) and metacinnabar (β-HgS). Chem. Geol. 240, 313–325.
Horvat, M., Lupšina, V., Pihlar, B., 1991. Determination of total mercury in coal fly ash by gold amalgamation cold vapour atomic absorption spectrometry. Anal. Chim. Acta 243, 71–79.
Hsu-Kim, H., Kucharzyk, K.H., Zhang, T., Deshusses, M.A., 2013. Mechanisms regulating mercury bioavailability for methylating microorganisms in the aquatic environment: a critical review. Environ. Sci. Technol. 47, 2441–2456.
Jan, F.A., Ishaq, M., Khan, S., Ihsanullah, I., Iahmad, I., Shakirullah, M., 2010. A comparative study of human health risk via consumption of food crops grown in wastewater irrigated soil (Peshawar) and relatively clean water irrigated soil (lower Dir). J. Hazard. Mater. 179, 612–621.
Jonsson, S., Skyllberg, U., Nilsson, M.B., Westlund, P.-O., Shchukarev, A., Lundberg, E., Björn, E., 2012. Mercury methylation rates for geochemically relevant Hg^{II} species in sediments. Environ. Sci. Technol. 46, 11653–11659.
Jonsson, S., Skyllberg, U., Nilsson, M.B., Lundberg, E., Andersson, A., Björn, E., 2014. Differentiated availability of geochemical mercury pools controls methylmercury levels in estuarine sediment and biota. Nat. Commun. 5, 4624. https://doi https://doi.org/10.1038/ncomms5624.
Kim, C.S., Bloom, N.S., Rytuba, J.J., Brown, G.E., 2003. Mercury speciation by X-ray absorption fine structure spectroscopy and sequential chemical extractions: a comparison of speciation methods. Environ. Sci. Technol. 37, 5102–5108.
León-Cañedo, J.A., Alarcón-Silvas, S.G., Fierro-Sañudo, J.F.F., Rodríguez-Montes de Oca, G.A., Partida-Ruvalcaba, L., Díaz-Valdés, T., Páez-Osuna, F., 2019. Mercury and other trace metals in lettuce (*Lactuca sativa*) grown with two low-salinity shrimp effluents: accumulation and human health risk assessment. Sci. Total Environ. 650, 2535–2544.
Liang, L., Horvat, M., Cernichiari, E., Gelein, B., Balogh, S., 1996. Simple solvent extraction technique for elimination of matrix interferences in the determination of methylmercury in environmental and biological samples by ethylation-gas chromatography-cold vapor atomic fluorescence spectrometry. Talanta 43 (11), 1883–1888.
Liu, J., Feng, X., Qiu, G., Yao, H., Shang, L., Yan, H., 2011. Intercomparison and applicability of some dynamic and equilibrium approaches to determine methylated mercury species in pore water. Environ. Toxicol. Chem. 30 (8), 1739–1744.
Liu, J., Feng, X., Qiu, G., Anderson, C.W., Yao, H., 2012. Prediction of methyl mercury uptake by rice plants (*Oryza sativa* L.) using the diffusive gradient in thin films technique. Environ. Sci. Technol. 46 (20), 11013–11020.
Liu, Y.R., Yu, R.Q., Zheng, Y.M., He, J.Z., 2014a. Analysis of the microbial community structure by monitoring an Hg methylation gene (hgc A) in paddy soils along an Hg gradient. Appl. Environ. Microbiol. 80 (9), 2874–2879.
Liu, Y.R., Zheng, Y.M., Zhang, L.M., He, J.Z., 2014b. Linkage between community diversity of sulfate-reducing microorganisms and methylmercury concentration in paddy soil. Environ. Sci.Pollut.Res.Int. 21 (2), 1339–1348.
Manceau, A., Lemouchi, C., Enescu, M., Gaillot, A.C., Lanson, M., Magnin, V., Glatzel, P., Poulin, B.A., Ryan, J.N., Aiken, G.R., Gautier-Luneau, I., Nagy, K.L., 2015. Formation of mercury sulfide from Hg(II)-thiolate complexes in natural organic matter. Environ Sci Technol 49, 9787–9796.
Manceau, A., Wang, J., Rovezzi, M., Glatzel, P., Feng, X., 2018. Biogenesis of mercury-sulfur nanoparticles in plant leaves from atmospheric gaseous mercury. Environ. Sci. Technol. 52, 3935–3948.
Mazrui, N.M., Seelen, E., King'ondu, C.K., Thota, S., Awino, J., Rouge, J., Zhao, J., Mason, R.P., 2018. The precipitation, growth and stability of mercury sulfide nanoparticles formed in the presence of marine dissolved organic matter. Environ. Sci. Proc. Impacts 20, 642–656.
Meng, B., Feng, X., Qiu, G., Liang, P., Li, P., Chen, C., Shang, L., 2011. The process of methyl mercury accumulation in rice (*Oryza sativa* L.). Environ. Sci. Technol. 45 (7), 2711–2717.
Miretzky, P., Bisinoti, M.C., Jardim, W.F., Rocha, J.C., 2005. Factors affecting Hg (II) adsorption in soils from the Rio Negro basin (Amazon). Quím. Nova 28, 438–443.
National Health Commission of the People's Republic of China, 2015. Report on nutrition and chronic disease of Chinese residents. http://www.nhc.gov.cn/jkj/s5879.
Pham, A.L.T., Morris, A., Zhang, T., Ticknor, J., Levard, C., Hsu-Kim, H., 2014. Precipitation of nanoscale mercuric sulfides in the presence of natural organic matter: structural properties, aggregation, and biotransformation. Geochim. Cosmochim. Acta 133, 204–215.
Ravichandran, M., Aiken, G.R., Reddy, M.M., Ryan, J.N., 1998. Enhanced dissolution of cinnabar (mercuric sulfide) by dissolved organic matter isolated from the Florida Everglades. Environ. Sci. Technol. 32, 3305–3311.
Ravichandran, M., Aiken, G.R., Ryan, J.N., Reddy, M.M., 1999. Inhibition of precipitation and aggregation of metacinnabar (mercuric sulfide) by dissolved organic matter isolated from the Florida Everglades. Environ. Sci. Technol. 33, 1418–1423.
Rothenberg, S.E., Feng, X., 2012. Mercury cycling in a flooded rice paddy. J. Geophys. Res. 117, G03003.
Rothenberg, S.E., Feng, X., Zhou, W., Tu, M., Jin, B., You, J., 2012. Environment and genotype controls on mercury accumulation in rice (*Oryza sativa* L.) cultivated along a contamination gradient in Guizhou, China. Sci. Total Environ. 426, 272–280.
Schaefer, J.K., Morel, F.M.M., 2009. High methylation rates of mercury bound to cysteine by Geobacter sulfurreducens. Nat. Geosci. 2, 123–126.
Shetaya, W.H., Huang, J.H., Osterwalder, S., Mestrot, A., Bigalke, M., Alewell, C., 2019. Sorption kinetics of isotopically labelled divalent mercury ($^{196}Hg^{2+}$) in soil. Chemosphere 221, 193–202.
Skyllberg, U., Xia, K., Bloom, P.R., Nater, E.A., Bleam, W.F., 2000. Binding of mercury (II) to reduced sulfur in soil organic matter along upland-peat soil transects. J. Environ. Qual. 29, 855–865.
Slowey, A.J., 2010. Rate of formation and dissolution of mercury sulfide nanoparticles: the dual role of natural organic matter. Geochim. Cosmochim. Acta 74, 4693–4708.
Terzano, R., Santoro, A., Spagnuolo, M., Vekemans, B., Medici, L., Janssens, K., Göttlicher, J., Denecke, M.A., Mangold, S., Ruggiero, P., 2010. Solving mercury (Hg) speciation in soil samples by synchrotron X-ray microspectroscopic techniques. Environ. Pollut. 158, 2702–2709.
Thomas, S.A., Rodby, K.E., Roth, E.W., Wu, J., Gaillard, J.F., 2018. Spectroscopic and microscopic evidence of biomediated HgS species formation from Hg(II)-cysteine complexes: implications for Hg(II) bioavailability. Environ. Sci. Technol. 52, 10030–10039.
United States Environmental Protection Agency, 1998. Method 1630: Methyl Mercury in Water by Distillation, Aqueous Ethylation, Purge and Trap, and CVAFS. US Environmental Protection Agency, Washington, DC.
United States Environmental Protection Agency, 2002. Method 1631: Mercury in Water by Oxidation, Purge and Trap, and Cold Vapor Atomic Fluorescence Spectrometry. US Environmental Protection Agency, Washington, DC.
United States Environmental Protection Agency, 2017. IRIS, Integrated Risk Information System. https://www.epa.gov/iris.
Wang, C., Song, Z., Li, Z., Zhu, W., Li, P., Feng, X., 2019. Mercury speciation and mobility in salt slurry and soils from an abandoned chlor-alkali plant, Southwest China. Sci. Total Environ. 652, 900–906.
Wang, J.X., Feng, X.B., Anderson, C.W.N., Wang, H., Zheng, L.R., Hu, T.D., 2012a. Implications of mercury speciation in thiosulfate treated plants. Environ. Sci. Technol. 46, 5361–5368.
Wang, J.X., Feng, X.B., Anderson, C.W.N., Xing, Y., Shang, L.H., 2012b. Remediation of mercury contaminated sites - a review. J. Hazard. Mater. 221, 1–18.
Wang, J.X., Anderson, C.W.N., Xing, Y., Fan, Y., Xia, J., Shaheen, S.M., Rinklebe, J., Feng, X., 2018. Thiosulphate-induced phytoextraction of mercury in *Brassica juncea*: spectroscopic investigations to define a mechanism for Hg uptake. Environ. Pollut. 242, 986–993.
Wang, J.X., Xing, Y., Xie, Y., Meng, Y., Xia, J., Feng, X., 2019a. The use of calcium carbonate-enriched clay minerals and diammonium phosphate as novel immobilization agents for mercury remediation: spectral investigations and field applications. Sci. Total Environ. 646, 1615–1623.
Wang, J.X., Shaheen, S.M., Swertz, A.C., Rennert, T., Feng, X., Rinklebe, J., 2019b. Sulfur-modified organoclay promotes plant uptake and affects geochemical fractionation of

mercury in a polluted floodplain soil. J. Hazard. Mater. 371, 687–693.
Wang, S.Q., Zhong, T.Y., Chen, D.M., Zhang, X.Y., 2016. Spatial distribution of mercury (Hg) concentration in agricultural soil and its risk assessment on food safety in China. Sustainability 8, 795–807.
Waples, J.S., Nagy, K.L., Aiken, G.R., Ryan, J.N., 2005. Dissolution of cinnabar (HgS) in the presence of natural organic matter. Geochim. Cosmochim. Acta 69 (6), 1575–1588.
Wu, C., Wu, G., Wang, Z., Zhang, Z., Qian, Y., Ju, L., 2018. Soil mercury speciation and accumulation in rice (*Oryza sativa* L.) grown in wastewater-irrigated farms. Appl. Geochem. 89, 202–209.
Xing, Y., Wang, J., Xia, J., Liu, Z., Zhang, Y., Du, Y., Wei, W., 2019. A pilot study on using biochars as sustainable amendments to inhibit rice uptake of Hg from a historically polluted soil in a Karst region of China. Ecotoxicol. Environ. Saf. 170, 18–24.
Xu, X.L., Zhao, L.Y., Fang, H.Y., Guo, Q.Y., Wang, X., Yu, W.T., Fang, Y.H., Yu, D.M., 2017. Present situation of consumption and variation of cereal in China. Food Nutr Chin 23, 44–46 (In Chinese).
Yin, R.S., Gu, C.H., Feng, X.B., Hurley, J.P., Krabbenhoft, D.P., Lepak, R.F., Zhu, W., Zheng, L.R., Hu, T.D., 2016. Distribution and geochemical speciation of soil mercury in Wanshan Hg mine: effects of cultivation. Geoderma 272, 32–38.
Zhang, H., Feng, X.B., Larssen, T., Qiu, G.L., Vogt, R.D., 2010a. In inland China, rice, rather than fish is the major pathway for methylmercury exposure. Environ. Health Perspct. 118, 1183–1188.
Zhang, H., Feng, X., Larssen, T., Shang, L., Li, P., 2010b. Bioaccumulation of methylmercury versus inorganic mercury in rice (*Oryza sativa* L.) grain. Environ. Sci. Technol. 44, 4499–4504.
Zhang, T., Kim, B., Levard, C., Reinsch, B.C., Lowry, G.V., Deshusses, M.A., Hsu-Kim, H., 2012. Methylation of mercury by bacteria exposed to dissolved, nanoparticulate, and microparticulate mercuric sulfides. Environ. Sci. Technol. 46 (13), 6950–6958.
Zhu, W., Song, Y., Adediran, G.A., Jiang, T., Reis, A.T., Pereira, E., Skyllberg, U., Björn, E., 2018. Mercury transformations in resuspended contaminated sediment controlled by redox conditions, chemical speciation and sources of organic matter. Geochim. Cosmochim. Acta 220, 158–179.